

Cite this: *Phys. Chem. Chem. Phys.*, 2011, **13**, 20199–20207

www.rsc.org/pccp

PAPER

## $^2\text{H}$ NMR calculations on polynuclear transition metal complexes: on the influence of local symmetry and other factors†

Iker del Rosal,<sup>a</sup> Torsten Gutmann,<sup>b</sup> Bernadeta Walaszek,<sup>c</sup> Iann C. Gerber,<sup>a</sup> Bruno Chaudret,<sup>a</sup> Hans-Heinrich Limbach,<sup>c</sup> Gerd Buntkowsky<sup>d</sup> and Romuald Poteau<sup>\*a</sup>

Received 26th June 2011, Accepted 9th September 2011

DOI: 10.1039/c1cp22081k

It is now well-known that  $^2\text{H}$  solid-state NMR techniques can bring a better understanding of the interaction of deuterium with metal atoms in organometallic mononuclear complexes, clusters or nanoparticles. In that context, we have recently obtained experimental quadrupolar coupling constants and asymmetry parameters characteristic of deuterium atoms involved in various bonding situations in ruthenium clusters, namely  $\text{D}_4\text{Ru}_4(\text{CO})_{12}$ ,  $\text{D}_2\text{Ru}_6(\text{CO})_{18}$  and other related compounds [Gutmann *et al.*, *J. Am. Chem. Soc.*, 2010, **132**, 11759], which are model compounds for edge-bridging ( $\mu\text{-H}$ ) and face-capping ( $\mu_3\text{-H}$ ) coordination types on ruthenium surfaces. The present work is in line with density functional theory (DFT) calculations of the electric field gradient (EFG) tensors in deuterated organometallic ruthenium complexes. The comparison of quadrupolar coupling constants shows an excellent agreement between calculated and observed values. This confirms that DFT is a method of choice for the analysis of deuterium NMR spectra. Such calculations are achieved on a large number of ruthenium clusters in order to obtain quadrupolar coupling constants characteristic of a given coordination type: terminal-D,  $\eta^2\text{-D}_2$ ,  $\mu\text{-D}$ ,  $\mu_3\text{-D}$  as well as  $\mu_4\text{-D}$  and  $\mu_6\text{-D}$  (*i.e.* interstitial deuterides). Given the dependence of such NMR parameters mainly on local symmetry, these results are expected to remain valid for large assemblies of ruthenium atoms, such as organometallic ruthenium nanoparticles.

### 1 Introduction

Metal nanoparticles (NPs) are the subject of intense investigations due to their ability to present new properties, intermediate between clusters and bulk materials.<sup>1–5</sup> In the context of catalysis, the reactivity of metal NPs is still an open question, particularly the nature of reactive sites and of intermediate surface species and the way to tune their selectivity. Getting knowledge of their structure would be very helpful, but their structure may often not be characterized at the same level as well-defined molecular species. Solid-state NMR spectroscopy has recently proved to be successful for elucidating the presence of mobile hydrides on the surface of ruthenium NPs,<sup>6</sup> whereas the

combination of this method with desorption techniques has given insights on the reactivity of these NPs.<sup>7</sup> In most cases, spectra assignment is not obvious, so that there is a need for providing reference data. Quantum chemistry can contribute to secure the attribution of spectroscopic NMR information in the case where assignment cannot be fully achieved by experimental means, as we have recently done in the case of hydrides.<sup>8–10</sup> The coordination of hydrogen to metal nanoparticles synthesized by organometallic techniques is especially important. These surface hydrides seem to be involved in hydrogenation processes, insofar as they can react with other compounds coordinated at the surface of the NPs. While hydrogen binding to a clean metal surface is now well understood both by experiments and periodic density functional theory (DFT) calculations,<sup>11–14</sup> the NP case needs further investigations. From a more general point of view, quadrupolar solid-state NMR properties of resonant nuclei can be tackled by quantum chemistry methods and can yield structural information, in synergy with experiments.<sup>15,16</sup> The present paper is specifically devoted to the calculation of quadrupolar parameters of deuterium atoms on ruthenium clusters and to the role of local symmetry on these NMR data.

All possible hydride adsorption sites on a clean Ru(001) surface, which is only a model for hcp Ru NPs, are summarized in Fig. 1. Co-ligands adsorbed on the surface as well as defects

<sup>a</sup> Université de Toulouse, INSA, UPS, CNRS, LPCNO, 135 avenue de Rangueil, F-31077 Toulouse, France. E-mail: romuald.poteau@univ-tlse3.fr; Fax: 0033 561559697; Tel: 0033 561559664

<sup>b</sup> Université de Toulouse, UPS, CNRS, LCC, 205 route de Narbonne, F-31077 Toulouse Cedex, France

<sup>c</sup> Institut für Physikalische und Theoretische Chemie, Freie Universität Berlin, Takustr. 3, D-14195 Berlin, Germany

<sup>d</sup> Eduard-Zintl-Institut für Anorganische und Physikalische Chemie, Technische Universität Darmstadt, Petersenstr. 20, D-64287 Darmstadt, Germany

† Electronic supplementary information (ESI) available: Computational details. See DOI: 10.1039/c1cp22081k

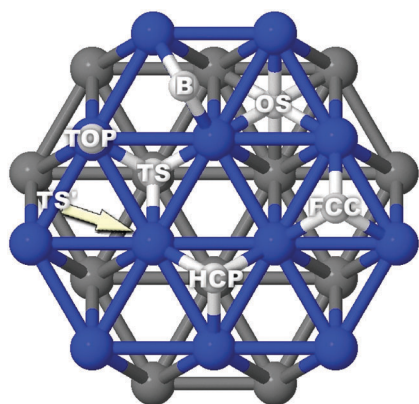


**Fig. 1** Top view of possible adsorption sites on a Ru(001) surface. TOP = terminal-H; B = edge-bridging H; FCC = face-capping H above an octahedral building block; HCP = face-capping H above a tetrahedral building block; TS = interstitial H in a tetrahedral site; TS' = alternative tetrahedral site for an interstitial H; OS = interstitial H in an octahedral site.

can play a role on the coordination mode, the mobility and the properties of surfacic and subsurfacic H atoms. DFT calculations achieved for co-adsorbed H and CO species have shown that H is strongly affected by co-adsorption.<sup>11</sup> While FCC adsorption sites are thermodynamically preferred by H atoms, the co-existence of H and CO involves that H is forced to populate sites close to CO at sufficiently high coverage. Given that the energy difference between FCC and HCP surfacic adsorption sites on clean Ru(001) surfaces is less than 3 kcal mol<sup>-1</sup>,<sup>13,14,17</sup> the study of all possible adsorption sites is necessary.

At the opposite end of the size scale, we have recently analyzed the role of ligands (L) on the electronic, spectroscopic (IR and <sup>1</sup>H NMR) and structural properties of several H<sub>m</sub>Ru<sub>4</sub>L<sub>n</sub> and [H<sub>m</sub>Ru<sub>6</sub>(CO)<sub>18</sub>]<sup>(2-m)-</sup> clusters.<sup>18</sup> Several structures compete in a relatively narrow energy range for H<sub>4</sub>Ru<sub>4</sub>L<sub>m</sub>, but the most stable one depends on the ligand type. Although in all these low-energy structures hydride atoms adopt edge-bridging or face-capping positions, it is possible to study terminal positions in geometries with higher energy as well as subsurfacic hydrides in tetrahedral or octahedral sites. Moreover, the structure and stability of small clusters can be analyzed *via* bonding schemes which lead in particular to Mingos–Wade rules.<sup>19,20</sup> Tetrahedral and octahedral structures belong, respectively, to the *nido* and *closo* family of clusters, so that Ru<sub>4</sub> and Ru<sub>6</sub> clusters obeying the rules should exhibit 60 and 86 valence electrons. We also considered strongly electron-deficient H<sub>4</sub>Ru<sub>4</sub>(CO)<sub>9</sub> clusters, in order to roughly mimic electron-deficient surfaces of NPs. While infra-red data do not clearly exhibit the spectroscopic signature of hydrides, comparison of experimental and theoretical <sup>1</sup>H NMR properties appears to be partially a probe of their coordination mode. Although μ-H cannot be easily distinguished from μ<sub>3</sub>-H or subsurfacic μ<sub>4</sub>-H due to similar shieldings, it seems possible to identify subsurfacic μ<sub>6</sub>-H and terminal hydrides which turn out to be significantly unshielded.<sup>10,18</sup> Nevertheless, the wide chemical shift range observed for a given coordination mode does not allow us to make safe assignments, unless theoretical calculations are involved. Since periodic boundary calculations with plane wave basis sets are tools of choice for the description of organometallic compounds, calculation of NMR properties

with standard periodic DFT packages is desirable in order to bring another point of view. However, such tools are still not easily available, although one should quote the existence of the methodology developed by Pickard and Mauri.<sup>21,22</sup>

In addition to <sup>1</sup>H NMR, we have also achieved a joint experimental and theoretical determination of <sup>2</sup>H solid-state NMR quadrupolar parameters of deuterons in ruthenium organometallic complexes. In the solid state, the deuterium NMR spectrum is determined by the electric field gradient (EFG) at the deuterium nuclear site. The EFG is a tensor quantity with a trace of zero. The deuterium quadrupole coupling constant, C<sub>Q</sub>, given by the largest diagonal element of the tensor, is a sensitive function of the metal–hydride bond geometry and interaction. The asymmetry parameter, η<sub>Q</sub>, is related to the shape of the EFG.<sup>23</sup> The agreement with experiments turned out to be excellent.<sup>9</sup> This synergy between experiments and theory seemed in particular very promising for elucidating the coordination mode of deuterides with metal atoms as well as the origin (Ru–D vs. D in ligands) of all the features of experimental spectra. Note also the existence of such theoretical/experimental combination in ref. 24, although the agreement between both techniques was not so good, probably owing to a basis set not large enough and to experiments performed at too high temperatures. As confirmed by DFT calculations, quadrupolar coupling constants are somewhat different for terminal-deuterium atoms and η<sup>2</sup>-dideuterides.<sup>9,23</sup> However one has to pay attention to temperature effects which may significantly modify experimental quadrupolar splittings, as it is the case with the rotational motion of D<sub>2</sub> ligands.<sup>25</sup> In the case of such dynamic features in transition metal complexes, the comparison with theoretical quadrupole parameters gives hints to motion processes. Experimental <sup>2</sup>H solid-state NMR techniques were also recently applied to small ruthenium clusters in order to investigate quadrupolar coupling constants for typical two-fold and three-fold coordination schemes.<sup>10</sup> Preliminary DFT results were also given in order to help in the interpretation of the experimental results obtained for D<sub>4</sub>Ru<sub>4</sub>(CO)<sub>12</sub>, D<sub>2</sub>Ru<sub>6</sub>(CO)<sub>18</sub>, [DRu<sub>6</sub>(CO)<sub>18</sub>]<sup>-</sup> and [D<sub>3</sub>Ru<sub>6</sub>(CO)<sub>18</sub>]<sup>+</sup> and have confirmed the remarkable agreement between theory and experiments.

Since such bonding can also be encountered at the surface of nanoparticles, this previous study was a first step to the solid-state NMR joint experimental/*in silico* spectroscopic characterization of deuterium adsorbed on the surface of metal nanoparticles obtained by an organometallic approach. In the present paper, DFT quadrupolar splittings of deuterons involved in all the organometallic ruthenium clusters considered in ref. 18 are calculated, with the same successful computational strategy used for mononuclear ruthenium complexes.<sup>9</sup> Such compounds exhibit a larger variety of coordination modes for deuterides (terminal, edge-bridging, face-capping), more or less hindered by co-ligands with various electron donor or π acceptor properties. Other clusters have been added to this representative set of [Ru<sub>4</sub>] and [Ru<sub>6</sub>] clusters.<sup>26</sup> This study thus allows us to theoretically define a frequency range in order to have a correlation between C<sub>Q</sub> and each bonding situation. We also show that C<sub>Q</sub> is strongly dependent on local symmetry, whereas the metal has no influence on C<sub>Q</sub> in these H<sub>4</sub>M<sub>4</sub>(CO)<sub>12</sub> clusters. While the electronic effect of ligands do

not either modify the quadrupolar parameters, we will show that steric effects can distort the local symmetry and significantly alter them. Although all the computed data are intended to estimate  $^2\text{H}$  solid state NMR frequency domains as a function of the possible coordination of D in molecules, clusters, NPs and on surfaces, some of these results may be of interest in the cluster field, whose chemistry has again attracted interest over the last decade.<sup>27</sup>

## 2 Results

### 2.1 Tetranuclear ruthenium complexes

**2.1.1  $\text{D}_4\text{Ru}_4(\text{CO})_{12}$ .** According to X-ray analysis,<sup>28</sup> the geometry of this cluster consists in a distorted tetrahedral core. The carbonyl groups are staggered with respect to the metal–metal edges and the  $D_{2d}$  symmetry of this molecule is consistent with edge-bridging hydrides. One of our previous studies on this topic<sup>18</sup> showed that the lowest isomer ( $\mathbf{1}^{\text{CO}}$ ) is consistent with these experimental data.

We had also found a large number of higher energy structures on the potential energy surface (PES) derived from  $\mathbf{1}^{\text{CO}}$ . Most of these isomers are shown in Fig. 2: a structure with  $C_s$  symmetry ( $\mathbf{2}^{\text{CO}}$ ), which is localized only 6.3 kcal mol<sup>-1</sup> above  $\mathbf{1}^{\text{CO}}$ , a  $T_d$  structure with four face-capping hydrides ( $\mathbf{3}^{\text{CO}}$ ), a  $C_{3v}$  structure with three edge-bridging hydrides and one  $\mu_3\text{-H}$  atom ( $\mathbf{4}^{\text{CO}}$ ), a  $C_1$  structure which exhibits three  $\mu\text{-H}$ , one terminal hydride and an edge-bridging carbonyl ligand ( $\mathbf{5}^{\text{CO}}$ ), a high-energy structure with four terminal hydrides ( $\mathbf{6}^{\text{CO}}$ ) and a low-energy structure with an interstitial hydride ( $\mathbf{7}^{\text{CO}}$ ).

Note that according to  $^1\text{H}$  liquid state NMR measurements,<sup>29</sup> a H-flipping mechanism about H-occupied Ru–Ru edges was proposed, with an activation energy of  $18 \pm 2$  kJ mol<sup>-1</sup>, *i.e.*  $4.4 \pm 0.5$  kcal mol<sup>-1</sup>. According to our calculations, the lowest accessible transition state leads to a structure,  $\mathbf{1}'^{\text{CO}}$ , very close to  $\mathbf{1}^{\text{CO}}$  both in terms of geometry and energy (Fig. 3). This distorted  $D_{2d}$  structure is almost degenerate with  $\mathbf{1}^{\text{CO}}$  ( $\Delta E$  0.2 kcal mol<sup>-1</sup>,  $\Delta_r G^\circ$  0.0 kcal mol<sup>-1</sup>). Since such a small energy difference is below the expected accuracy of

DFT, identification of the most stable isomer is hazardous. Deuterium atoms in  $\mathbf{1}^{\text{CO}}$  are out of the  $\text{Ru}_3$  faces with angles of  $36^\circ$  between the  $\text{Ru}_3$  and the Ru–D–Ru planes, whereas in  $\mathbf{1}'^{\text{CO}}$  they tend to get closer to the plane defined by a triangular  $\text{Ru}_3$  face, with an angle of  $23^\circ$ . The transition state between these structures lies 3 kcal mol<sup>-1</sup> above the two minima. This  $\Delta_r G^\circ$  value turns out to be close to the experimental activation energy found by Harding *et al.*<sup>29</sup> However, while these authors have proposed a flipping mechanism of the bridging hydrogen at higher temperatures, according to DFT calculations, it is not a 2-site H-flip about Ru–Ru edges. Actually, the imaginary normal mode of vibration which characterizes  $\text{TS}_2$  involves an adjustment of the position of deuterides, facilitated by the partial rotation of  $\text{Ru}(\text{CO})_3$  fragments. The nature of minima and transition states on the PES around  $\mathbf{1}^{\text{CO}}$  is not in favor of the H-flipping motion postulated by Harding *et al.* Interestingly, previous experiments led to a higher activation energy value of 16.1 kcal mol<sup>-1</sup>,<sup>30</sup> recalculated to be 7.7 kcal mol<sup>-1</sup> by Harding *et al.*, and interpreted as a dynamic process involving either the  $\text{Ru}_4\text{H}_4$  core as a whole or a concerted motion of the hydrides over the surface of the  $\text{Ru}_4$  core. Incidentally, the corrected value is in close agreement with the isomerization between the  $\mathbf{1}^{\text{CO}}/\mathbf{1}'^{\text{CO}}$  average structure and  $\mathbf{2}^{\text{CO}}$ . It is however not straightforward to conclude in favor of one mechanism or the other and such a case deserves thorough experimental investigations or new explorations of the PES by means of other WFT theoretical methods. Pay attention that periodic boundary calculations (Fig. 4) provide the same low-lying minima and transition states, so that they do not question gas-phase calculations ( $\mathbf{2}^{\text{CO}}$  and  $\text{TS}_1$  are located 4 kcal mol<sup>-1</sup> and 6.2 kcal mol<sup>-1</sup> above  $\mathbf{1}^{\text{CO}}$ ).

Quadrupolar coupling constants  $C_Q$  and asymmetry parameters  $\eta_Q$  are given in Table 1 for deuterated compounds. Preliminary calculations have already been performed on  $\mathbf{1}^{\text{CO}}$  at the DFT-B3LYP level of calculation, with an averaged relativistic effective potential on Ru and triple-zeta quality basis sets on other atoms.<sup>10</sup> These  $C_Q$  values, although higher than those calculated at the present level of calculation by 14 kHz, represent the experimental value at 173 K ( $C_Q \approx 67$  kHz) in a good way. The asymmetry parameters  $\eta_Q$  calculated at both levels of calculations are in excellent agreement

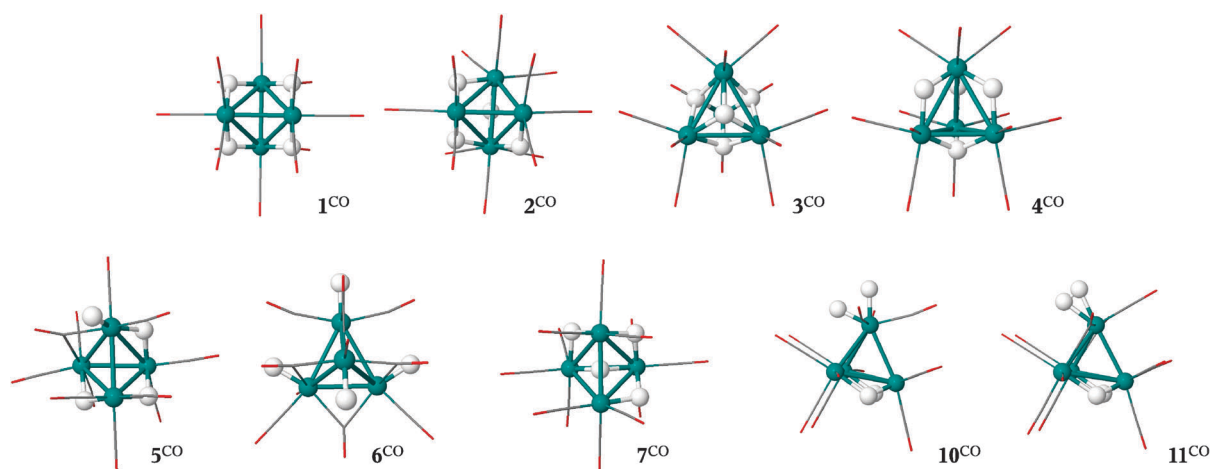
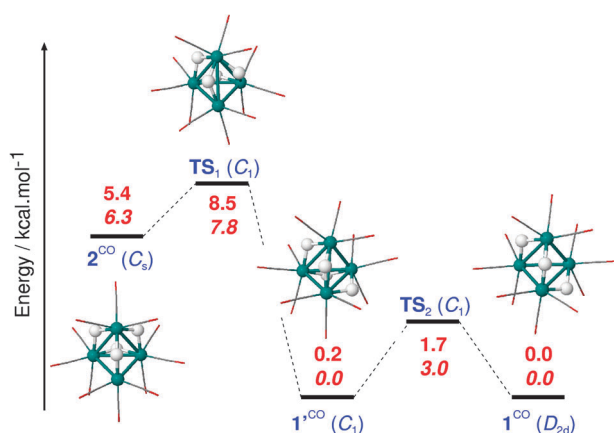
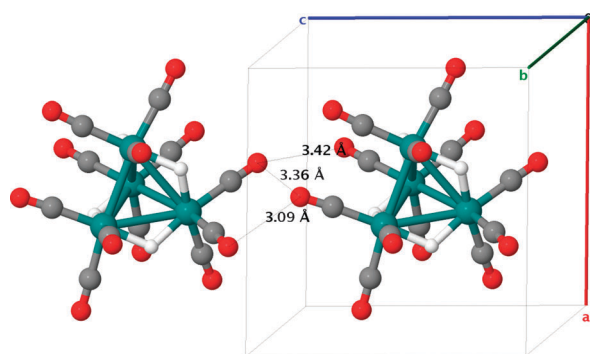


Fig. 2 Structures for  $\text{H}_4\text{Ru}_4(\text{CO})_{12}$  (after ref. 18 for clusters 1–7).



**Fig. 3** Isomerization pathway between  $2^{\text{CO}}$  and  $1^{\text{CO}}$ . The symmetry group is given between parenthesis. The energies are given with respect to the lowest structure (first line: electronic energy  $\Delta E$ ; second line: Gibbs free energy  $\Delta_r G^\circ$ ). The geometry of  $\text{TS}_2$ , not very different from  $1'^{\text{CO}}$  and  $1^{\text{CO}}$ , is not shown here.



**Fig. 4** Unit cell plot for  $\text{Ru}_4\text{H}_4(\text{CO})_{12}$ , corresponding to the optimized DFT-PBE crystal structure of  $1^{\text{CO}}$ , with close contact distances between two neighboring clusters.

with the experimental value ( $\eta_{\text{Q}} \approx 0.67$  in all cases). Incidentally, the  $C_{\text{Q}}$  value calculated in this work (67 kHz) coincides with experimental data.

Terminal-D atoms are all characterized by  $C_{\text{Q}} \approx 88$  kHz, *i.e.* very close to the values calculated for mononuclear ruthenium complexes, excepted  $\text{Cp}^*\text{RuD}_3\text{PPh}_3$  which is slightly higher by 10 kHz.<sup>9</sup>  $C_{\text{Q}}$  decreases upon increasing the coordination of ruthenium atoms, with *ca.* 67 kHz for  $\mu$ -D and only 8–25 kHz for  $\mu_3$ -D atoms. Edge-bridging atoms in  $7^{\text{CO}}$  are characterized by low values for  $C_{\text{Q}}$ , in the range [46–51 kHz]. This lowering seems to be related to the presence of an interstitial deuterium atom, which alters the electronic structure of Ru–H bonds. A significantly low value for  $C_{\text{Q}}$  is also found for one  $\mu$ -D in  $2^{\text{CO}}$ , probably owing to the shortening of the Ru–Ru bond. The last two species, namely  $10^{\text{CO}}$  and  $11^{\text{CO}}$ , exhibit interesting coordination features. Two edge-bridging hydrides and two H atoms coordinated to the same ruthenium atom are present in both compounds, which are minima on the PES. A predissociated  $\eta^2\text{-H}_2$  ligand is present in  $11^{\text{CO}}$  ( $d_{\text{HH}}$  0.87 Å), whereas the H–H bond length is significantly elongated in  $10^{\text{CO}}$  (1.67 Å). Again, as can be seen in Table 1,  $\mu$ -D atoms have characteristic  $C_{\text{Q}}$  and  $\eta_{\text{Q}}$  parameters, although the asymmetry parameter is slightly higher than in previous clusters. The quadrupolar parameters found for terminal deuteride atoms in  $10^{\text{CO}}$  are also very close to those previously found for  $6^{\text{CO}}$ . Finally, the values calculated for the  $\eta^2\text{-D}_2$  ligand in  $11^{\text{CO}}$  are in the upper limit of the characteristic domain defined according to calculations performed for mononuclear ruthenium complexes.<sup>9</sup>

**2.1.2  $\text{D}_4\text{Ru}_4(\text{C}_6\text{H}_6)_4$  and  $[\text{D}_4\text{Ru}_4(\text{C}_6\text{H}_6)_4]^{2+}$ .**  $[\text{H}_4\text{Ru}_4(\text{C}_6\text{H}_6)_4]^{2+}$  ( $3^{\text{C}_6\text{H}_6, 2+}$ ) is a *nido* electron-deficient cluster containing 58 electrons and face-capping hydrides. Its structure, slightly distorted with respect to the 60-electrons  $T_d$  cluster ( $3^{\text{C}_6\text{H}_6}$ , Fig. 5a), was experimentally characterized.<sup>31</sup> Quadrupolar coupling constants have been calculated for both

**Table 1** Comparison of  $C_{\text{Q}}$  (in kHz) and  $\eta_{\text{Q}}$  for several isomers of  $\text{H}_4\text{Ru}_4(\text{CO})_{12}$ . The energies, in  $\text{kcal mol}^{-1}$ , are given relatively to  $1^{\text{CO}}$  (see also ref. 18).  $\mu_4\text{-D}$  refers to a deuterium subsurface atom, whereas T stands for terminal atoms

Isomer	$\Delta_r G^\circ$	D position	$C_{\text{Q}}$	$\eta_{\text{Q}}$	Isomer	$\Delta_r G^\circ$	D position	$C_{\text{Q}}$	$\eta_{\text{Q}}$
$1^{\text{CO}}$	0.0	$\mu$	66	0.67	$6^{\text{CO}}$	43.2	T	86	0.03
$1'^{\text{CO}}$	0.0	$\mu$	65	0.69	$7^{\text{CO}}$	11.4	T( $\times 2$ )	90	0.05
			66	0.68			T	89	0.01
			66	0.68			$\mu$	51	0.87
			67	0.67			$\mu$	46	0.98
$2^{\text{CO}}$	6.3	$\mu$	70	0.60	$10^{\text{CO}}$	29.3	$\mu$	46	0.98
			54	0.81			$\mu$	46	0.98
			71	0.58			$\mu_4$	37	0.73
			68	0.62			T	88	0.04
$3^{\text{CO}}$	30.0	$\mu_3$	8	0.06	$11^{\text{CO}}$	26.4	T	88	0.07
			74	0.55			$\mu$	63	0.75
$4^{\text{CO}}$	13.0	$\mu$	25	0.09	$\eta^2\text{-D}_2$		$\mu$	63	0.75
			$\mu_3$				$\mu$	61	0.74
$5^{\text{CO}}$	18.9	$\mu$	59	0.11	$\mu$	61	0.74		
			63	0.69					
			66	0.64					
			91	0.09					

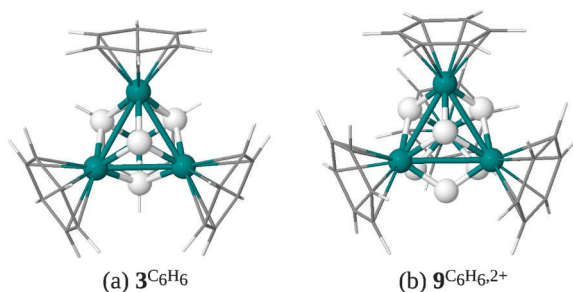


Fig. 5 Structure for (a)  $H_4Ru_4(C_6H_6)_4$ ; (b)  $[H_6Ru_4(C_6H_6)_4]^{2+}$ .

Table 2 Comparison of  $C_Q$  (in kHz) and  $\eta_Q$  for  $[D_4Ru_4(C_6H_6)_4]^{n+}$  and  $[D_6Ru_4(C_6H_6)_4]^{2+}$

Isomer	Ru–D		C–D		
	D position	$C_Q$	$\eta_Q$	$C_Q$	$\eta_Q$
$3^{C_6H_6}$	$\mu_3$	7	0.00	207	0.08
$3^{C_6H_6,2+}$	$\mu_3$	15	0.61	201	0.07
		16	0.60		
		16	0.59		
		14	0.68		
$9^{C_6H_6,2+}$	$\mu$	50	0.95	201	0.06
	$\mu_3$	34	0.12		

compounds, in order to check if electron deficiency influence the  $C_Q$  value. This is not the case, as it is shown in Table 2. Similarly to the property calculated for  $3^{CO}$ ,  $C_Q$  is very small:  $\sim 7$  kHz for the neutral and  $\sim 15$  kHz for the cationic clusters. On the other hand,  $\eta_Q$ , equal to zero in the highly symmetric case ( $3^{C_6H_6}$ ), significantly increases for the cationic compound, in relation with a Jahn–Teller effect which rules the geometry of  $3^{C_6H_6,2+}$ . While a dependence of  $C_Q$  on Ru–Ru bond lengths has been observed for  $\mu$ -D, this property varies little with the geometry of the capped face. As a matter of fact, the Ru–Ru distances are 2.91 Å in  $3^{CO}$ , and only 2.77 Å in  $3^{C_6H_6}$ , but Ru–D quadrupolar coupling constants differ by 1 kHz only. Likewise, the desymmetrization of the capped  $Ru_3$  face ( $2 \times 2.84$  Å and 2.59 Å) in  $3^{C_6H_6,2+}$  with respect to  $3^{C_6H_6}$  does not involve a large increase of  $C_Q$ , whereas it has a dramatic effect on  $\eta_Q$ , in relation with a strong modification of the shape of the EFG. The three Ru–( $\mu_3$ -D) distances could be a relevant index of local asymmetry. They are similar in the present case, with two values close to 1.84 Å, the last one being more elongated (1.89 Å). In summary, these results confirm that quadrupolar coupling constants are characteristic of the local symmetry, and not dependent on the ligands coordinated to ruthenium atoms. Finally, note that C–D quadrupolar coupling constants are still close to 200 kHz for both compounds.

**2.1.3  $[D_6Ru_4(C_6H_6)_4]^{2+}$ .** It is also a *nido* electron-saturated cluster. It has been experimentally synthesized and characterized,<sup>32</sup> with a hydride/Ru ratio greater than 1. This compound exhibits three edge-bridging hydrides and three face-capping hydrides ( $9^{C_6H_6,2+}$ , Fig. 5b). The quadrupolar parameters are reported in Table 2.  $C_Q$  for the face-capping deuterides is significantly higher than those previously found for  $3^{CO}$  and  $3^{C_6H_6,2+}$  with a value close to 34 kHz, although it remains below the characteristic domain of edge-bridging hydrides (46–74 kHz).  $\mu$ -D are likewise characterized by a value

(50 kHz) close to the lower bound of the  $\mu$  domain. Both results can be explained by geometrical considerations. As a matter of fact the  $Ru_3$  faces on which  $\mu_3$ -D are coordinated are not equilateral triangles. As a consequence the three Ru–D distances are not identical (1.73 Å and  $2 \times 1.92$  Å). This distortion is significantly more important than for  $3^{C_6H_6,2+}$  and may explain the increase of  $C_Q$ . In summary, the  $Ru_3$ D fragment does not have a perfect threefold rotational symmetry. In contrast, edge bridging deuterides are symmetrically bound to ruthenium atoms. The small value calculated for  $C_Q$  seems rather related to an unusually short Ru–Ru bond length, 2.88 Å, whereas it is 2.98 Å in  $1^{CO}$  and 3.03 Å in  $4^{CO}$ . C–D are again characterized by  $\Delta\nu_Q$  ca. 150 kHz.

## 2.2 Hexanuclear ruthenium complexes

Experimental  $^2H$  solid-state NMR MAS measurements performed on the  $D_2Ru_6(CO)_{18}$  cluster as well as preliminary DFT calculations at the B3LYP level of theory on the  $D_2Ru_6(CO)_{18}$  and  $[DRu_6(CO)_{18}]^-$  clusters have been reported in a previous article.<sup>10</sup>

**2.2.1  $D_2Ru_6(CO)_{18}$ .** Two  $\mu_3$ -H are localized on opposite faces of the  $Ru_6$  octahedron,<sup>33</sup> which can be considered as a prototype of hydrides adsorbed on a FCC site ( $13'$ , Fig. 6a). This compound belongs to the  $D_{3d}$  symmetry group, which means that the H atoms are located on the threefold symmetry axis, and that they cap the equilateral  $Ru_3$ -triangles. The Ru–H distances in this complex are slightly higher than in  $3^{CO}$  (1.89 Å vs. 1.87 Å) and the Ru–Ru distances for the two  $Ru_3$  capped faces are also larger than previously found in  $3^{CO}$  (2.96 Å vs. 2.91 Å). Although  $C_Q$  remains small (25 kHz), it is found to be higher than calculated for  $3^{CO}$ ,  $3^{C_6H_6}$  and  $3^{C_6H_6,2+}$ . It is similar to the value calculated for  $9^{C_6H_6,2+}$ , but probably for different reasons, since the local three-fold symmetry in  $13'$  is not observed in  $9^{C_6H_6,2+}$ . 25 kHz could be a typical value for  $\mu_3$ -D adsorbed on FCC sites, that is somewhat different from  $\mu_3$ -D adsorbed on HCP sites.

Concerning asymmetry parameters, very small values ( $\eta \leq 0.06$ ) are found in the present case, owing to the local three-fold symmetry. However, we have checked on a totally unsymmetric isomer which possesses carbonyl groups randomly oriented that  $\eta_Q$  is very dependent upon geometry distortions. In that isomer, which is only few kcal mol<sup>-1</sup> above the symmetric geometry,  $\mu_3$ -D are still characterized by quadrupolar coupling constants close to 27 kHz, but the asymmetry parameter now culminates to 0.6.

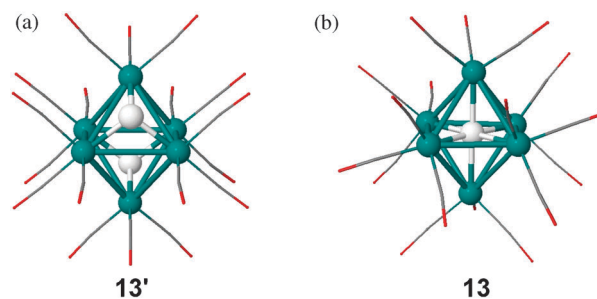


Fig. 6 Structure for  $H_2Ru_6(CO)_{18}$ ,  $13'$  and  $[HRu_6(CO)_{18}]^-$ ,  $13$ .

**2.2.2 [DRu<sub>6</sub>(CO)<sub>18</sub>]<sup>-</sup>.** This compound (**13**, Fig. 6b), first mentioned in 1980, has been characterized by X-ray analysis as well as by <sup>1</sup>H NMR, variable-temperature <sup>13</sup>C NMR and infrared techniques.<sup>34</sup> In addition, its presence has recently been observed as a side product in a H<sub>2</sub>Ru<sub>6</sub>(CO)<sub>18</sub> sample.<sup>10</sup> Thanks to this previous joint DFT/experimental study, we have shown that NMR data are consistent with an interstitial hydride atom. Such cluster happens to be the prototype of a H ligand inside an octahedral site (OS site in Fig. 1). It is interesting to notice that <sup>1</sup>H NMR may allow us to identify subsurface OS hydrides. H is located at the center of the octahedron. The quadrupolar coupling constant  $C_Q$  is very weak (2 kHz) due to the octahedral Ru<sub>6</sub> environment of the H which yield an EFG close to zero at the H position.  $C_Q$  is significantly sensitive to a reduction in symmetry: the quadrupolar coupling constant increases by 31 kHz if H lies closer to an edge by 0.2 Å with respect to its optimal position, whereas it increases only by 17 kHz when H is moved 0.2 Å closer to a vertex. While the asymmetry parameter  $\eta_Q$  is almost the same (*i.e.* 0.1) as far as one local  $C_4$  symmetry axis is kept, it significantly increases to 0.7 when the four-fold symmetry is broken.

**2.2.3 [D<sub>3</sub>Ru<sub>6</sub>(CO)<sub>18</sub>]<sup>+</sup>.** The <sup>1</sup>H NMR spectrum of D<sub>2</sub>Ru<sub>6</sub>(CO)<sub>18</sub>, recorded in a previous paper,<sup>10</sup> exhibits a weak signal group, which was attributed to a decomposition product, namely [H<sub>3</sub>Ru<sub>6</sub>(CO)<sub>18</sub>]<sup>+</sup>. Quadrupolar interactions of the deuterated species, similar to those observed for D<sub>2</sub>Ru<sub>6</sub>(CO)<sub>18</sub>, were estimated to be  $C_Q = 25 \pm 4$  kHz at rt, with an asymmetry parameter  $\eta_Q = 0.2 \pm 0.2$ .<sup>10</sup> We found three isomers within 4 kcal mol<sup>-1</sup> on the potential energy surface of that cluster (Fig. 7), two of them (**14a** and **14b**) being almost degenerate and connected *via* a low-lying transition state ( $\Delta G^\ddagger$  3.6 kcal mol<sup>-1</sup>). Since **14b** exhibits an interstitial  $\mu_6$ -H, it means that a surface hydrogen can easily undergo a surface–subsurface motion, even at low temperature.  $C_Q$  and  $\eta_Q$  values in **14a** are calculated to be 23.4, 35.0 and 43.1 kHz and 0.22, 1.00 and 0.97 respectively. Surface deuterides in **14b** exhibit similar  $C_Q$  values, albeit lower (13.1 kHz, with  $\eta_Q$  0.51 and 0.38), whereas the  $\mu_6$ -D is shifted from the center of the octahedral site and is thus characterized by a somewhat large  $C_Q$  value (26.3 kHz, with  $\eta_Q$  0.13). Another isomer, **14c**, incidentally found during the optimization process, exhibits three  $\mu_3$ -H as well as a  $\mu_3$ -CO and lies only  $\Delta G^\circ$  1.0 kcal mol<sup>-1</sup> above **14a**. Pay attention that  $C_Q$  values in **14c**, calculated to be 43.7, 45.3 and 46.4 kHz (with  $\eta_Q$  0.65, 0.63 and 0.15), are

among the highest found for  $\mu_3$ -H. We will get back to this case in the discussion section.

### 2.3 An example of electron-deficient cluster: D<sub>2</sub>Ru<sub>4</sub>(CO)<sub>9</sub>

This is a prototype of 52e electron-deficient cluster, which exhibits one  $\mu$ -H which has roughly the same neighborhood than any hydride in H<sub>4</sub>Ru<sub>4</sub>(CO)<sub>12</sub> and one  $\mu_3$ -H which is alone above a face since three carbonyl groups have been suppressed (Fig. 8). This specific electron-counting has been considered in ref. 18 according to electron-deficiency at the surface of ruthenium NPs. According to our <sup>1</sup>H NMR calculations, such surface hydrides are expected to be strongly unshielded. However, there is no significant effect on quadrupolar coupling constants.  $C_Q$  for the  $\mu_3$ -D and  $\mu$ -D (17 kHz and 53 kHz) are similar to the previous values found for  $\mu_3$  deuterides. Whereas the chemical shift is very sensitive to electron-count, owing to obvious screening effects, the quadrupolar coupling constant seems to rather depend on local symmetry only. The asymmetry parameter is much more sensitive, with  $\eta_Q > 0.8$  in both cases.

### 2.4 Other ruthenium clusters

In addition to carbonyl and  $\eta^6$ -C<sub>6</sub>H<sub>6</sub> clusters, quadrupolar parameters have been calculated for all the other compounds considered in ref. 18, *i.e.* tetrahedral clusters with Lewis base ligands PH<sub>3</sub>, PF<sub>3</sub> and AsH<sub>3</sub>. All the  $C_Q$  values calculated in this study are reported in Fig. 9, together with the values previously calculated for mononuclear ruthenium complexes<sup>9</sup> and those calculated for deuterides adsorbed on pristine Ru(001) surfaces.<sup>14</sup>  $C_Q$  values are gathered in a column according to a given coordination mode, clearly showing domains which in general do not overlap. However, with a domain spreading from  $\mu$ -D to terminal-D, dideuterides are less easy to identify. Furthermore, bearing in mind that tunneling effects have been proven to occur in  $\eta^2$ -D<sub>2</sub> transition metal complexes,<sup>25,35</sup> the experimental range is expected to be wider. Terminal-D and  $\mu$ -D domains weakly overlap, owing to **1**<sup>PF<sub>3</sub></sup> and **2**<sup>PF<sub>3</sub></sup> which exhibit Ru<sub>4</sub>(H)<sub>4</sub> moieties significantly

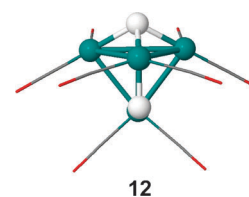


Fig. 8 Structure for ( $\mu_2$ -H)( $\mu_3$ -H)Ru<sub>4</sub>(CO)<sub>9</sub>.

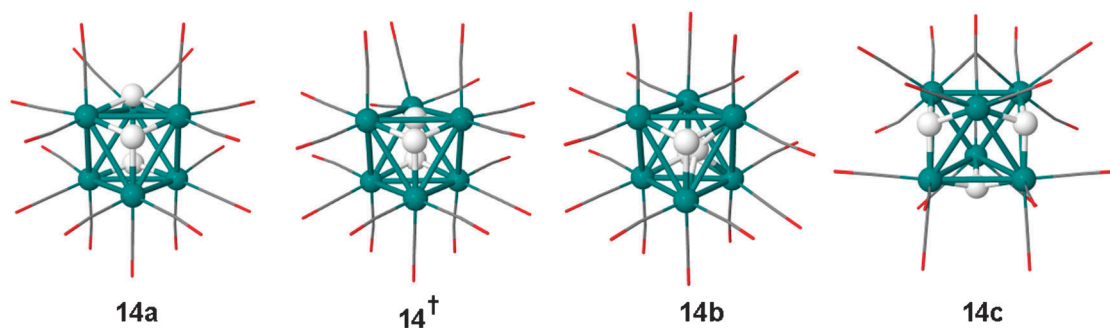
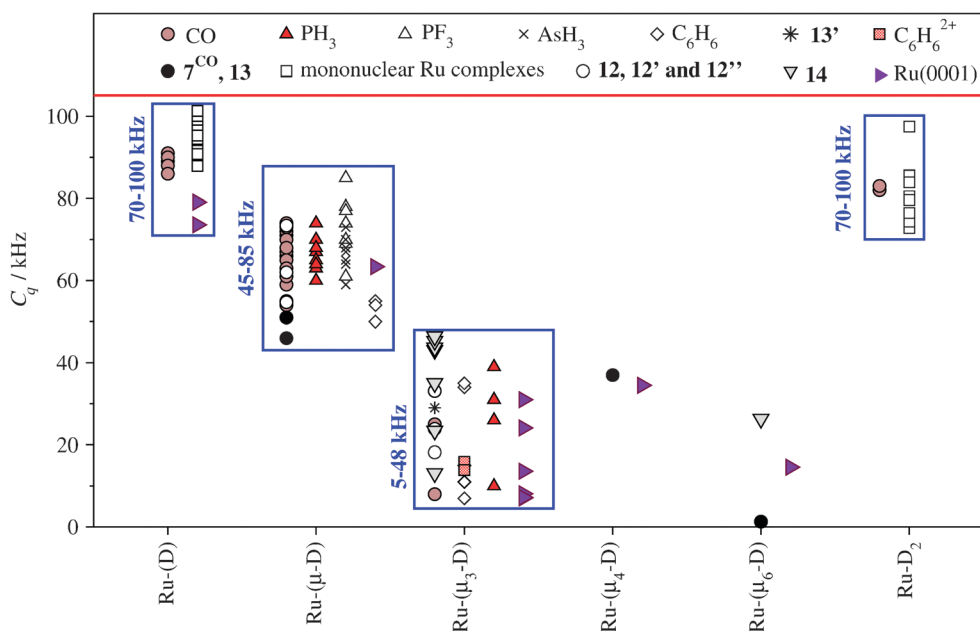


Fig. 7 Isomers for [Ru<sub>6</sub>(CO)<sub>18</sub>H<sub>3</sub>]<sup>+</sup>.



**Fig. 9**  $C_Q$  values calculated in this work for deuterides in ruthenium complexes, clusters, and adsorbed on slabs (values for Ru(0001) and mononuclear ruthenium complexes are taken from refs. 9 and 14).

distorted away from  $D_{2d}$  and  $C_s$  symmetry.  $\mu_3$ -D are characterized by low values of quadrupolar coupling constants, which range from 7 kHz to *ca.* 39 kHz ( $3^{PH_3}$ ). Interstitial deuterides in tetrahedral ( $\mu_4$  or TS) and octahedral ( $\mu_6$  or OS) sites have been considered. TS deuterides cannot be distinguished from  $\mu_3$ -D, with a value also close to the lower bound of the  $\mu$  domain. The OS deuteride in **13'** coincides with the inversion center of this  $D_{3d}$  structure and is characterized by an extremely low value for  $C_Q$ . As regards  $\eta_Q$ , it is systematically comprised between 0.6 and 0.8 for isomers **2**. While it has a low value in the case of  $3^{CO}$  and  $3^{C_6H_6}$ , it is very large in  $3^{PH_3}$ , owing to the local distortion induced by the steric hindrance between  $PH_3$  functional groups.

### 2.5 Other metal atoms

This section aims at evaluating if the domain characteristic of a given type of coordination is still valid for other metal atoms. Recently, deuterium variable-temperature  $T_1$  measurements have been performed for a series of rhenium carbonyl clusters containing doubly and triply bridging deuterides. We have more particularly considered  $(\mu_3\text{-D})_4Re_4(CO)_{12}$ , a 56e cluster, for which quadrupolar coupling constants were experimentally found to be 21.8 kHz.<sup>36</sup> Our calculations agree well with these experimental data, with  $C_Q$  17 kHz. As expected for a 3-fold coordination type,  $\eta_Q$  is small ( $0.04 \pm 0.01$ ). Although slightly higher than in  $3^{C_6H_6,2+}$  or  $3^{CO}$ ,  $C_Q$  remains in the  $\mu_3$  domain. Calculations have also been performed for the isoelectronic  $(\mu_3\text{-D})_4Tc_4(CO)_{12}$  cluster. Quadrupolar parameters are almost insensitive to the metal atom, with  $C_Q$  18 kHz and  $\eta_Q$   $0.03 \pm 0.01$ . Finally, two 60e clusters have also been considered, namely  $(\mu\text{-D})_4Fe_4(CO)_{12}$  and  $(\mu\text{-D})_4Os_4(CO)_{12}$ . The quadrupolar parameters, calculated to be  $C_Q$  67 kHz for both compounds and  $\eta_Q$  0.68 and 0.74, respectively, are almost identical to those calculated for  $1^{CO}$ , although the M–M and M–H bond lengths differ (M–M: 2.88 Å and 2.99 Å for  $[Os_4]$ , 2.57 Å and

2.72 Å for  $[Fe_4]$ ; M–H: 1.80 Å for  $[Os_4]$ , 1.62 Å for  $[Fe_4]$ ). Although it should be extensively checked in more cases, it tends to indicate that quadrupolar parameters do not depend much on the metal.

## 3 Discussion

$C_Q$  values calculated for all mentioned clusters<sup>26</sup> are reported in Fig. 9. For the sake of completeness and in order to have an overview for all coordination possibilities, the values previously calculated<sup>9</sup> for terminal-D and  $\eta^2\text{-D}_2$  species are also given, together with D atoms adsorbed on Ru(0001) surfaces.<sup>14</sup> We shall now try to understand the origin of the scattering of  $C_Q$  values in the  $\mu$  and  $\mu_3$  domains. In both cases, we have considered the possible influence of various geometry parameters. Edge-bridging deuterium atoms usually form an isosceles triangle with the Ru–Ru side, *i.e.* they are localized in the symmetry plane of the tetrahedral unit which is orthogonal to the edge. Two peculiar positions can be identified. The first one is localized in the local  $C_2$  axis of the tetrahedral core (such as in  $1^{CO}$ ) the second one coplanar with one  $Ru_3$  face (such as in  $1^{PH_3}$ ). We have carefully checked that the distortion of the local  $C_2$  symmetry upon going from the ideal  $\mu$  position to the coplanar position cannot account for the scattering of  $C_Q$  values observed in the range [47–87 kHz]. With the noticeable exception of the interstitial-H-containing isomer  $7^{CO}$ , it seems more related to the Ru–Ru bond length of the capped edge, as can be seen in Fig. 10a. As regards  $\mu_3$ -D, we have stated in previous sections that  $C_Q$  may be related to the deviation of D with respect to three-fold rotation symmetry. Such situation is involved by a distortion of the capped face as well as steric crowding of ligands which primarily act on the position of D above the face. We propose to evaluate this deviation by calculating for each  $\mu_3$ -D encountered in all compounds the standard deviation ( $\sigma_N$ ) of the three Ru–H bond lengths.

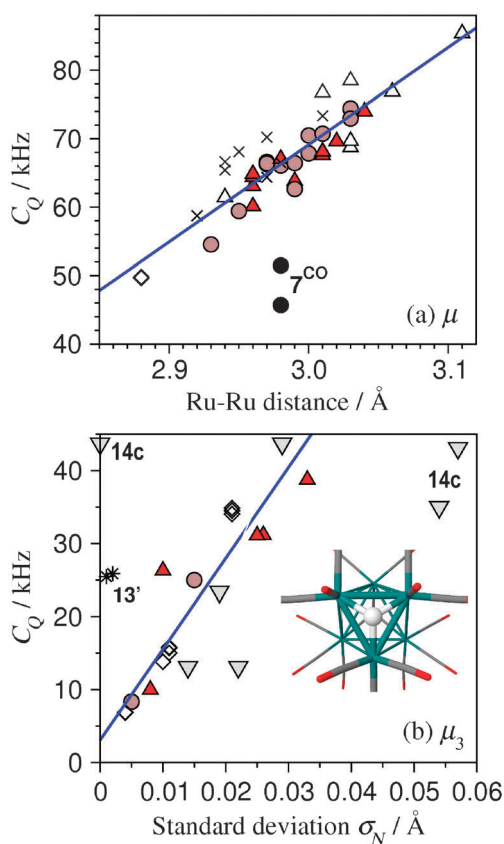


**Fig. 10** Analysis of the dispersion observed for  $C_Q$ . (a) Edge-bridging deuterides:  $C_Q$  seems to be mainly related to the Ru–Ru bond length (set of values calculated for  $1^{CO}$ ,  $1^{PF_3}$ ,  $1^{PH_3}$ ,  $1^{AsH_3}$ ,  $2^{CO}$ ,  $2^{PF_3}$ ,  $2^{PH_3}$ ,  $2^{AsH_3}$ ,  $4^{CO}$ ,  $4^{PH_3}$ ,  $5^{CO}$ ,  $7^{CO}$ ,  $9^{C_6H_6,2^+}$ ); (b) face-capping deuterides:  $C_Q$  seems to be mainly related to the centering of D above the triangular face (see text for details; set of values calculated for  $3^{CO}$ ,  $3^{C_6H_6}$ ,  $3^{C_6H_6,2^+}$ ,  $3^{PH_3}$ ,  $4^{CO}$ ,  $4^{PH_3}$ ,  $9^{C_6H_6,2^+}$ ,  $13'$  and  $14a-c$ ).

$C_Q$  is plotted as a function of  $\sigma_N$  in Fig. 10b, thus showing a convincing linear correlation. The more noticeable exception is observed for **14c**, *i.e.* one  $[Ru_6(CO)_{18}D_3]^+$  isomer. A new point of view is highlighted in Fig. 10b. A  $Ru(CO)_3$  subunit has rotated in **14c** with respect to **13** or **13'** in order to facilitate the adsorption of a third D atom. Such motion involves a reduction in local symmetry from three-fold rotation to reflection symmetry for all D atoms. While one of them is adsorbed on an equilateral triangular facet (small  $\sigma_N$  value), its  $C_Q$  value is very high (43.7 kHz) and overlaps with the  $\mu$  domain, owing to this reduction of symmetry of the local surroundings. As regards OS sites, the variation of the H position in **13** (section 3.2.2) shows that  $C_Q$  and  $\eta_Q$  are sensitive to symmetry reduction. A displacement from OS to an edge breaks the  $C_4$  and inversion symmetry, thus involving a significant increase of  $C_Q$  and  $\eta_Q$ . A displacement from OS to a vertex also breaks inversion symmetry but keeps one four-fold axis. The asymmetry parameter remains low accordingly, whereas  $C_Q$  slightly increases.

## 4 Conclusion

In summary, according to DFT calculations performed on mononuclear ruthenium complexes, organometallic clusters and Ru(0001) slabs,  $C_Q$  in the range of:

- [70–100] kHz can be assigned to Ru–(D). This is consistent with experimental data, as already shown in a previous article,<sup>9</sup>

- [45–85] kHz can be assigned to Ru–( $\mu$ -D), according to the Ru–Ru bond length. This is in good agreement with  $^2H$  MAS NMR data obtained for  $Ru_4D_4(CO)_{12}$ ,<sup>10</sup>

- [5–50] kHz can be assigned to Ru–( $\mu_3$ -D), in agreement with the quadrupolar coupling constants obtained for  $D_2Ru_6(CO)_{18}$  and  $[D_3Ru_6(CO)_{18}] + [Ru_6D_3(CO)_{18}]^+$ .<sup>10</sup> The highest  $C_Q$  values are expected to be observed for  $\mu_3$ -D either moved away from the 3-fold symmetry axis by co-adsorbed ligands—it is for example the case on Ru(0001) surfaces with high coverage values—either when the local 3-fold symmetry is broken by the local orientation of co-adsorbed ligands—such as observed for **14c**,

- [0–5] kHz can be assigned to interstitial Ru–( $\mu_6$ -D) ideally located at the inversion center. It is very well possible to observe such deuterons by  $^2H$  NMR, it was indicated in the  $[HRu_6(CO)_{18}]^-$  case by a narrow signal with no spinning side bands.  $C_Q$  values close to zero are thus a very clear fingerprint of interstitial deuterons, together with their unshielded  $^1H$  NMR chemical shift.<sup>10</sup>  $C_Q$  is however sensitive to the distance from the inversion center and can significantly increase up to *ca.* 25 kHz, as calculated for **14b**.

- [70–100] kHz can be assigned to Ru–( $\eta^2$ -D<sub>2</sub>), according to the strength of the metal  $\rightarrow \sigma^*(H_2)$  back-donation. Mind that owing to tunneling effect,<sup>25</sup> the measured values are expected to cover a larger range than calculated.

-  $C_Q$  values close to 40 kHz can be assigned to Ru–( $\mu_4$ -D), *i.e.* subsurface deuterium atoms, albeit there is no experimental evidence. Such a value is found both for  $Ru_4D_4(CO)_{12}$  ( $7^{CO}$ ) and for D adsorbed in a TS site in Ru(0001) slabs. Given the local 3-fold symmetry,  $\mu_4$ -D cannot be distinguished from  $\mu_3$ -D by their  $C_Q$  value, nor by their large  $\eta_Q$  value which also characterizes strongly asymmetric  $\mu_3$ -D.

The very good agreement between DFT and experimental quadrupolar parameters has also been checked in the case of a 56e rhenium cluster, namely  $D_4Re_4(CO)_{12}$ . More generally, the calculations performed on other  $D_4M_4(CO)_{12}$  clusters ( $M = Fe, Os, Tc$ ) suggest that the frequency domains given in this paper should not depend much on the metal.

Quadrupolar parameters primarily depend on local symmetry: the highest the symmetry, the lowest the quadrupolar coupling constant  $C_Q$ . Variations in  $C_Q$  and  $\eta_Q$  as a function of external factors remain moderate, thus allowing us to define characteristic domains which slightly overlap according to the symmetry reduction and the metal–metal bond length. We have also considered several hydrogenated  $[Ru_n]$  clusters with different co-adsorbed ligands. While the steric hindrance of the ligands may alter the symmetry and induce an increase of the quadrupolar parameters, their electronic donor/acceptor effect does not involve a variation of  $C_Q$  and  $\eta_Q$ . The 56e rhenium cluster as well as the  $H_2Ru_4(CO)_9$  case suggest  $C_Q$  is not sensitive to the electron count, provided that this does not have a dramatic effect on the local symmetry and geometry.

There are two interesting by-products of this study, both related to the exploration of the potential energy surface of some clusters. One is the very low-lying transition state between a surface  $\mu_3$  coordination site and an octahedral

inner site. Even at low temperature, H atoms can easily penetrate in such OS sites, just below the surface. The second one is the isomerization pathway of  $\text{H}_4\text{Ru}_4(\text{CO})_{12}$ , in relation with an experimental debate in the literature.<sup>29,30</sup> Although exploring the potential energy surface around the lowest isomer is not as powerful as simulating a spectrum by means of molecular dynamics, it provides relevant clues about the possible relation between dynamics and NMR data.

Among other theoretical NMR studies devoted to different nuclei in organometallic complexes<sup>37</sup> or in solids,<sup>38</sup> it was recently shown that DFT calculations of chemical shieldings of protons in ruthenium clusters are fairly accurate.<sup>10,18,39</sup>  $^2\text{H}$  NMR, together with DFT calculations of EFG tensors, is also a powerful approach for elucidating the coordination of H with metal atoms (see also ref. 9 and 10). These combined theoretical/experimental studies should be considered with interest for a safe assignation of the experimental features of diamagnetic organometallic compounds, such as organometallic ruthenium complexes,<sup>40</sup> clusters<sup>10</sup> or NPs.<sup>6,7</sup>

## Acknowledgements

Financial support by the Deutsche Forschungsgemeinschaft under contracts BU 911/12-1,2 is gratefully acknowledged. We also thank the CALcul en MIDI-Pyrénées (CALMIP, project P0611) as well as the CINES (project pcn6211) for generous allocations of computer time.

## References

- 1 *Clusters and Colloids: From Theory to Applications*, ed. G. Schmid, VCH Publishers, Inc., Weinheim, Germany, 1994.
- 2 C. N. R. Rao, G. U. Kulkarni, P. J. Thomas and P. P. Edwards, *Chem. Soc. Rev.*, 2000, **29**, 27–35.
- 3 *Nanoscale Materials in Chemistry*, ed. K. J. Klabunde, Wiley-Interscience, New-York, 2001.
- 4 *Metal Nanoparticles: Synthesis Characterization & Applications*, ed. D. L. Fedlheim and C. A. Foss, Jr., Marcel Dekker, New-York, 2002.
- 5 *Nanoparticles. From theory to application*, ed. G. Schmid, Wiley-VCH, Weinheim, Germany, 2004.
- 6 T. Pery, K. Pelzer, G. Buntkowsky, K. Philippot, H. H. Limbach and B. Chaudret, *ChemPhysChem*, 2005, **6**, 605–607.
- 7 J. García-Antón, M. R. Axet, S. Jansat, K. Philippot, B. Chaudret, T. Pery, G. Buntkowsky and H.-H. Limbach, *Angew. Chem., Int. Ed.*, 2008, **47**, 2074–2078.
- 8 L. A. Truffandier, I. del Rosal, B. Chaudret, R. Poteau and I. C. Gerber, *ChemPhysChem*, 2009, **10**, 2939–2942.
- 9 I. del Rosal, T. Gutmann, L. Maron, F. Jolibois, K. Philippot, B. Chaudret, B. Wakaszek, H. H. Limbach, R. Poteau and G. Buntkowsky, *Phys. Chem. Chem. Phys.*, 2009, **11**, 5657–5663.
- 10 T. Gutmann, B. Walaszek, X. Yeping, M. Wächter, I. del Rosal, A. Grünberg, R. Poteau, R. Axet, G. Lavigne, B. Chaudret, H.-H. Limbach and G. Buntkowsky, *J. Am. Chem. Soc.*, 2010, **132**, 11759–11767.
- 11 I. M. Ciobica, A. W. Kleyn and R. A. V. Santen, *J. Phys. Chem. B*, 2003, **107**, 164–172.
- 12 K. Kostov, W. Widdra and D. Menzel, *Surf. Sci.*, 2004, **560**, 130–144.
- 13 L. Xu, H. Xiao and X. Zu, *Chem. Phys.*, 2005, **315**, 155–160.
- 14 I. D. Rosal, L. Truffandier, R. Poteau and I. C. Gerber, *J. Phys. Chem. C*, 2011, **115**, 2169–2178.
- 15 J. Cuny, S. Messaoudi, V. Alonzo, E. Furet, J.-F. Halet, E. Le Fur, S. E. Ashbrook, C. J. Pickard, R. Gautier and L. Le Polles, *J. Comput. Chem.*, 2008, **29**, 2279–2287.
- 16 J. Cuny, E. Furet, R. Gautier, L. Le Polles, C. J. Pickard and J.-B. d. de Lacaillerie, *ChemPhysChem*, 2009, **10**, 3320–3329.
- 17 M. Y. Chou and J. R. Chelikowsky, *Phys. Rev. B: Condens. Matter*, 1989, **39**, 5623.
- 18 I. del Rosal, F. Jolibois, L. Maron, K. Philippot, B. Chaudret and R. Poteau, *Dalton Trans.*, 2009, 2142–2156.
- 19 T. Albright, J. Burdett and M.-H. Whangbo, *Orbital interactions in chemistry*, John Wiley and Sons, Inc., New-York, 1985.
- 20 D. M. P. Mingos and D. J. Wales, *Introduction to cluster chemistry*, Prentice-Hall, Inc, Englewood Cliffs, NJ, 1990.
- 21 C. J. Pickard and F. Mauri, *Phys. Rev. B: Condens. Matter*, 2001, **63**, 245101.
- 22 M. d’Avezac, N. Marzari and F. Mauri, *Phys. Rev. B: Condens. Matter*, 2007, **76**, 165122.
- 23 D. L. Bryce, G. M. Bernard, M. Gee, M. D. Lumsden, K. Eichele and R. E. Wasylshen, *Can. J. Anal. Sci. Spectrosc.*, 2001, **46**, 46–82.
- 24 V. I. Bakhmutov, C. Bianchini, F. Maseras, A. Lledos, M. Peruzzini and E. V. Vorontsov, *Chem.–Eur. J.*, 1999, **5**, 3318–3325.
- 25 G. Buntkowsky and H. H. Limbach, *J. Low Temp. Phys.*, 2006, **143**, 55–114.
- 26 A more detailed description of this set is given in the ESI† together with the computational details, rather than in the main paper, in order to lighten it.
- 27 G. Hogarth, S. E. Kabir and E. Nordlander, *Dalton Trans.*, 2010, **39**, 6153–6174.
- 28 R. D. Wilson, S. M. Wu, R. A. Love and R. Bau, *Inorg. Chem.*, 1978, **17**, 1271–1280.
- 29 R. A. Harding, H. Nakayama, T. Eguchi, N. Nakamura, B. T. Heaton and A. K. Smith, *Polyhedron*, 1998, **17**, 2857–2863.
- 30 S. Aime, R. Gobetto, A. Orlandi, C. J. Groombridge, G. E. Hawkes, M. D. Mantle and K. D. Sales, *Organometallics*, 1994, **13**, 2375–2379.
- 31 R. Gautier, F. Chérioux, G. Süß-Fink and J.-Y. Saillard, *Inorg. Chem.*, 2003, **42**, 8278–8282.
- 32 G. Süß-Fink, L. Plasseraud, A. Maise-François, H. Stoeckli-Evans, H. Berke, T. Fox, R. Gautier and J.-Y. Saillard, *J. Organomet. Chem.*, 2000, **609**, 196–203.
- 33 M. R. Churchill and J. Wormald, *J. Am. Chem. Soc.*, 1971, **93**, 5670–5677.
- 34 C. R. Eady, P. F. Jackson, B. F. G. Johnson, J. Lewis, M. C. Malatesta, M. McPartlin and W. J. H. Nelson, *J. Chem. Soc., Dalton Trans.*, 1980, 383–392.
- 35 F. Wehrmann, T. P. Fong, R. H. Morris, H.-H. Limbach and G. Buntkowsky, *Phys. Chem. Chem. Phys.*, 1999, **1**, 4033–4041.
- 36 T. Beringhelli, G. D’Alfonso, R. Gobetto, M. Panigati and A. Viale, *Organometallics*, 2005, **24**, 1914–1918.
- 37 J. Autschbach, *The Calculation of NMR Parameters in Transition Metal Complexes*, in *Density functional theory in inorganic chemistry*, ed. N. Kaltsoyannis and J. E. McGrady, Springer-Verlag, Berlin/Heidelberg, 2004, vol. 112, pp. 1–48.
- 38 T. Charpentier, *Solid State Nucl. Magn. Reson.*, 2011, **40**, 1–20.
- 39 I. del Rosal, L. Maron, R. Poteau and F. Jolibois, *Dalton Trans.*, 2008, 3959–3970.
- 40 B. Walaszek, A. Adamczyk, T. Pery, X. Yeping, T. Gutmann, N. d. S. Amadeu, S. Ulrich, H. Breitzke, H. M. Vieth, S. Sabo-Etienne, B. Chaudret, H.-H. Limbach and G. Buntkowsky, *J. Am. Chem. Soc.*, 2008, **130**, 17502–17508.